

SYNTHESIS REPORT

FOR PUBLICATION

CONTRACT N° : BRE2 - CT93 - 0548

PROJECT N° : BE 7228

TITLE : Active Control of Structural Vibration using Power
Transmission Methods

PROJECT
COORDINATOR : Institute of Sound and Vibration Research (ISVR - UK)

PARTNERS : Centre Technique des Industries Mecaniques (CETIM-FRANCE)
Technical University of Denmark (TUD - DENMARK)

Industrial Endorsers:
Centro Ricerche Fiat (CRF - ITALY)
Brueel & Kjaer (B & K - DENMARK)
Thomson Sintra ASM (TS ASM - FRANCE)

STARTING DATE : 01/01/94

DURATION : 36 MONTHS



PROJECT FUNDED BY THE EUROPEAN
COMMUNITY UNDER THE BRITE/EURAM
PROGRAMME

Active Control of Structural Vibration Using Power Transmission Methods (ASPEN)

S. J. Elliott*, P. Gardonio¹, A. M. David¹, R. J. Pinnington¹ and J. Garcia-Bonito¹

G.Pavic, and M. Besombes²

E.Henriksen³ and M. Ohlrich³

¹Institute of Sound & Vibration Research, University of Southampton,
Highfield, Southampton SO17 IBJ, U.K.

²CETIM, 52 Av F Louat, 60304 Senlis cedex, France

³Technical University of Denmark, Lyngby 28000, Denmark

ABSTRACT

The isolation of vibration through a system with multiple active mounts is discussed, in which each of the mounts can transmit vibration in several degrees of freedom. Theoretical models of the various parts of this system have been developed which includes a flexible receiving structure and distributed active mounts, and these models can be connected together to produce an overall theoretical description of a realistic active isolation system. Total transmitted power has been found to be an excellent criterion to quantify the effect of various control strategies in this model in which the contributions to the transmitted power in the various degrees of freedom can be clearly understood. It has also been found, however, that an active control system which minimises a practical estimate of transmitted power, calculated from the product of the axial forces and velocities under the mounts, can give a very poor performance in terms of reducing the total transmitted power, and can even increase it under some circumstances. Such a control system was also found to, be very sensitive to measurement errors and the presence of flanking paths, which give rise to the phenomena of “power circulation”. A more practical control strategy appears to be to minimise the weighted sum of squared forces and velocities below the mounts, which gives near-optimal performance in simulations. These theoretical results are supported by experiments with a real-time control system. The actuator and sensor requirements of such an active vibration control system are also discussed.

1. Introduction

Active control can provide good levels of vibration isolation in applications where conventional passive systems would be too bulky or heavy. In the past the actuators in such a system have been adjusted to minimise the **response** of the structure to which the isolation system is attached. The sum of the squared output from a large number of accelerometers may be minimised for example, as shown in Fig. 1(a), which is an estimate of the total kinetic energy in the receiving structure. An alternative approach would be to concentrate on the

structural power being transmitted through the isolators as shown in Fig. 1(b), and hence control the **excitation** of the receiving structure.

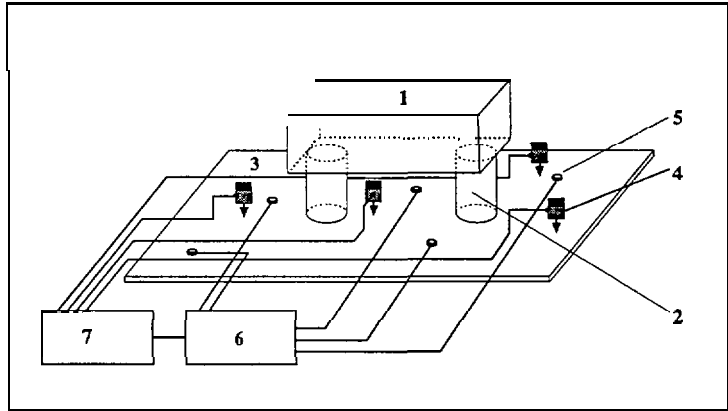


Fig. 1a: Conventional active vibration control system in which the **response** of the receiving structure is minimised.

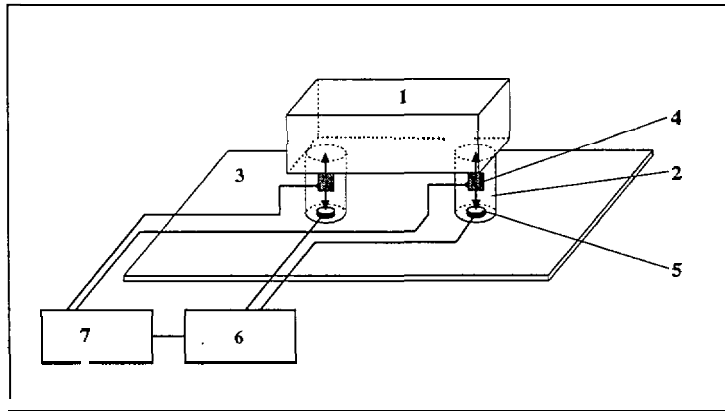


Fig. 1b: System investigated here in which the **excitation** of the receiving structure is minimised

This paper reports the results of a collaborative EC project in which the physical principles behind such a strategy were investigated. This initially involved a theoretical analysis of the active control of power transmission into infinite and finite systems [1, 2], which is not further discussed in this paper because of space constraints. We will concentrate here on reporting some of the other parts of the project, which included a study of different technologies for actuators and sensors, the development of a theoretical model of an active isolation system and a series of experiments in which the properties of all the parts of an active isolation were measured before finally measuring the performance of the whole system.

2. Actuators for Active Mounts

The design requirements for the actuator of an active mount can be understood from a simple analysis of its axial motion. We will assume that the actuator acts in parallel with the passive part of the mount, which avoids the need for excessive actuator requirements at the natural frequency of the source/mount system, [3]. If the secondary force is adjusted so that the total force transmitted through the mount due to the active and passive components is zero, then

the receiving structure will be not excited, so that the dynamic vibration of the source structure will be the same as if the source structure alone was floating freely in space. The stroke requirements of the actuator are thus equal to the free vibration displacement of the source structure. The secondary force generated by the actuator is then required to be equal to the free displacement of the source structure multiplied by the passive stiffness of the mount. For maximum efficiency, the ratio of the blocked force of the actuator to its free displacement must thus be matched to the stiffness of the passive part of the mount.

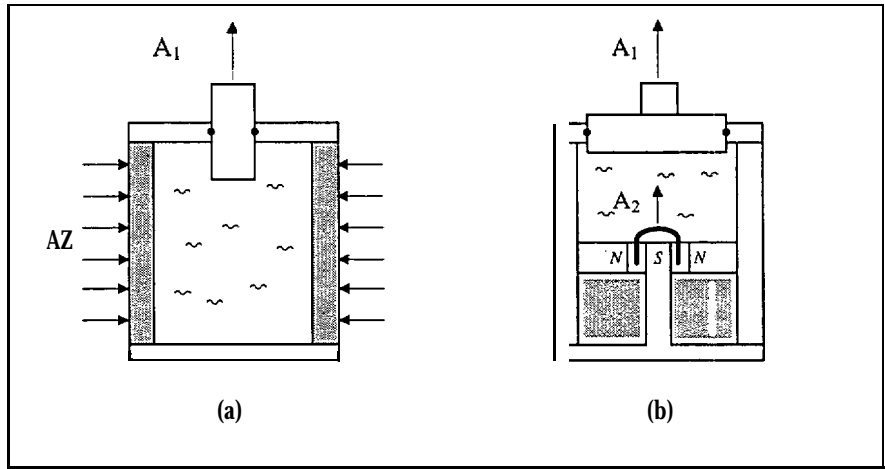


Fig. 2: Active mount designs in which either the displacement of a stiff actuators amplified hydraulically (a) or the force produced by a soft actuator is amplified hydraulically (b).

There are two main classes of actuator which could be used in such a system. The first class of actuators have a very high mechanical stiffness, and include piezoceramic and magnetostrictive devices. The stiffness of these devices will tend to be much higher than that of the required passive mount, and so to match the actuator to the passive system, some mechanism of displacement amplification must be used. One possible arrangement is illustrated in Fig. 2(a), which shows a piezoceramic cylinder of area A_2 enclosing a fluid chamber whose pressure acts on a piston with the smaller area A_1 [4]. The other class of actuator has a very low mechanical stiffness, e.g. piezoplastic or electromagnetic devices. If these are to be used to drive a passive isolator which has a higher stiffness, then some kind of force amplification device is required. An example of such a device is shown in Fig. 2(b) in which an electromagnetically driven piston of area A_2 drives a fluid chamber which acts on a plate of larger area A_1 . Considerable care needs to be taken with the design of such a device to prevent the fluid pressure from causing the elastic walls of the mount to bulge out, while allowing the elastic walls to take up the static load and give isolation for moment and shear excitations. The detailed design of such a device is described in [5].

3. Control Algorithms

In order to keep the design of the active isolator practical, it is only possible to incorporate sensors to measure the axial force and velocity acting on such a device. One of the main challenges of the project turned out to be to find ways of using these two measurements to form a cost function which could be minimised by a practical control algorithm, and which was robust to phase mismatch in the two sensors, and to flanking excitation.

The most obvious way of combining the force and velocity estimates together was to take their time-average product. This gives an estimate of the structural power being transmitted by the axial motion of the isolator. The vector of complex axial forces measured at a single frequency under the mounts can be written as

$$\mathbf{f} = \mathbf{f}_p + \mathbf{G}_f \mathbf{u} \quad (3.1)$$

where \mathbf{f}_p is the vector of forces due to primary source, \mathbf{u} is the vector of control inputs to the secondary actuators and \mathbf{G}_f is the matrix of transfer responses between the secondary actuators and the output of these sensors. Using similar notation, the vector of complex velocities at the bottom of a single mount can be written as

$$\mathbf{v} = \mathbf{v}_p + \mathbf{G}_v \mathbf{u}. \quad (3.2)$$

The sum of the time average products of the forces and velocities, which is the first cost function being considered here, can be written in the frequency domain as

$$J = \frac{1}{2} \text{Re} (\mathbf{f}^H \mathbf{v}) = \frac{1}{4} (\mathbf{f}^H \mathbf{v} + \mathbf{v}^H \mathbf{f}), \quad (3.3)$$

where the superscript H denotes the Hermitian, complex conjugate, transpose.

If a steepest descent algorithm is to be used in a feedforward system to adjust the secondary actuator, we require the derivative of this cost function with respect to the real and imaginary parts of \mathbf{u} , i.e. \mathbf{u}_R and \mathbf{u}_I , which can be written as

$$\mathbf{g} = \frac{\partial J}{\partial \mathbf{u}_R} + j \frac{\partial J}{\partial \mathbf{u}_I} = \frac{1}{2} (\mathbf{G}_v^H \mathbf{f} + \mathbf{G}_f^H \mathbf{v}). \quad (3.4)$$

Thus in contrast to the case in which the cost function is equal to the modulus squared value of only \mathbf{f} or \mathbf{v} , this derivative contains two terms which must be added together. The final steepest descent algorithm at the $n+1$ -th iteration is thus

$$\mathbf{u}(n+1) = \mathbf{u}(n) - \alpha (\mathbf{G}_v^H \mathbf{f} + \mathbf{G}_f^H \mathbf{v}) \quad (3.5)$$

where α is an adaptation coefficient. The real-time implementation of such a control algorithm has been studied by Laugesen [6] who also considered the effect of measurement phase errors on the behaviour of the algorithm in controlling the power being transmitted to a clamped-free beam. The results of this simulation are shown in Fig. 3, in which good control is obtained if the force and velocity are measured without any phase errors, but if a relative phase error of only 0.25 degrees is introduced into the measurements, then significant degradation in control performance occurs.

A new control strategy which arose as a result of the work reported here was prompted by the observation that the cancellation of axial force or velocity both gave good reductions in total transmitted power except at different sets of resonance frequencies.

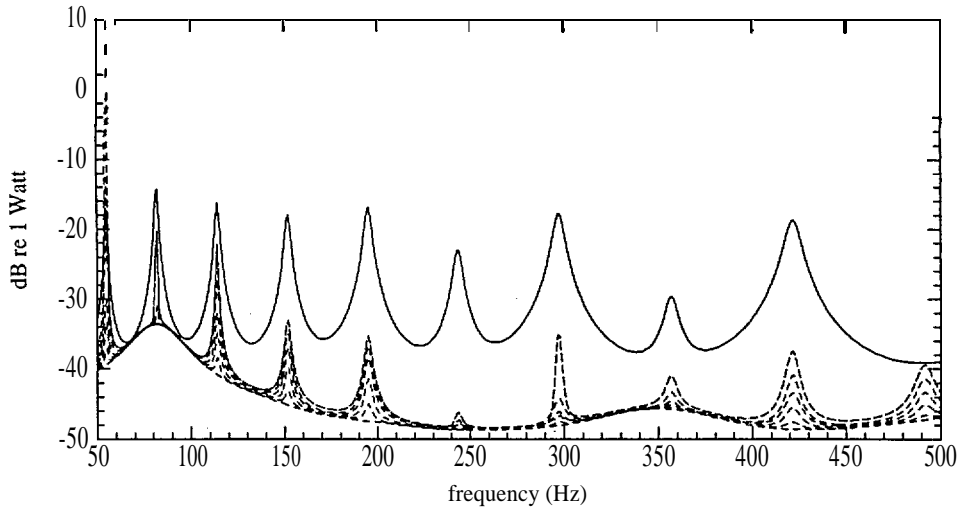


Fig. 3: Results of computer simulations of minimizing the cost function J , in which small phase errors are present in the relative measurement of force and velocity

Combining these two cost functions together, we obtain a new cost function of the form

$$\mathbf{J}_2 = \mathbf{v}^H \mathbf{v} + \mu \mathbf{f}^H \mathbf{f} \quad (3.6)$$

where μ is a constant which is not critical and was taken here to be equal to the squared mobility of an infinite plate of the same thickness as the receiving structure.

The steepest descent algorithm which minimises this new cost function (\mathbf{J}_2) is given by

$$\mathbf{u}(n+1) = \mathbf{u}(n) - \alpha (\mathbf{G}_v^H \mathbf{v} + \mu \mathbf{G}_f^H \mathbf{f}). \quad (3.7)$$

Despite the apparent similarity between this algorithm and that which minimises the product of force and velocity, equation (3.5), they are found in practice to have profoundly different effects in the system being controlled, as illustrated in the following section.

4. Theoretical Analysis of an Active Isolation System

The theoretical analysis of the isolation system involves a matrix description of the velocities and forces in all 6 degrees of freedom acting at the junctions between the source structure, the mounts and the receiving structure.

The full analysis is covered in detail by Gardonio *et al* [7], and is briefly described here before we discuss the results of a simulation for the special case in which there are only two mounts connecting the source to the receiving structure.

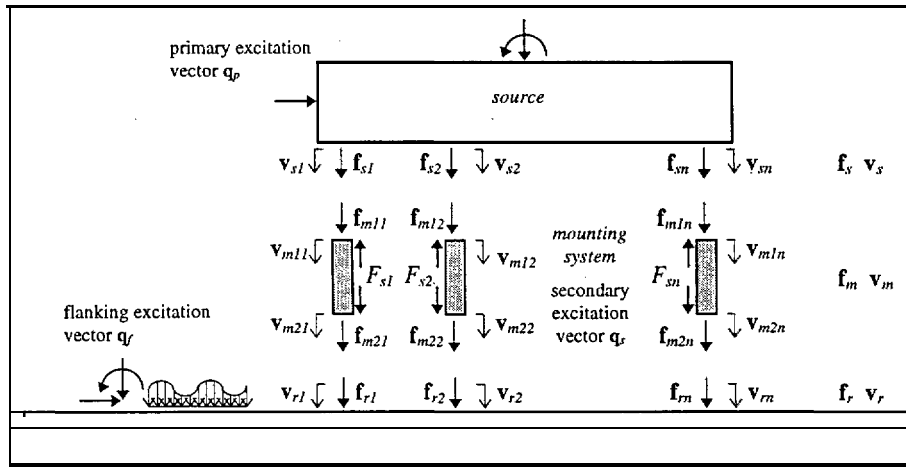


Fig. 4: Definition of forces and velocities for the active isolator

The dynamic response of source and receiving structures can be represented by their mobility matrices, \mathbf{M}_{s1} , \mathbf{M}_{s2} , \mathbf{M}_{r1} and \mathbf{M}_{r2} , so that

$$\mathbf{v}_s = \mathbf{M}_{s1} \mathbf{f}_s + \mathbf{M}_{s2} \mathbf{q}_p \quad (4.1)$$

$$\mathbf{v}_r = \mathbf{M}_{r1} \mathbf{f}_r + \mathbf{M}_{r2} \mathbf{q}_f \quad (4.2)$$

where \mathbf{v}_s and \mathbf{v}_r are vectors of the 6 linear and angular velocities at all the mounting points, \mathbf{f}_s and \mathbf{f}_r are the vectors of 6 linear forces and moments at all these mounting points, \mathbf{q}_p is the vector of primary forces and moments acting on the source structure and \mathbf{q}_f is a similar vector of forces and moments acting directly on the receiving structure due to flanking transmission. These two expressions can be grouped together into a single expression of the form

$$\mathbf{v}_{sr} = \mathbf{M}_{sr1} \mathbf{f}_{sr} + \mathbf{M}_{sr2} \mathbf{q}_{pf} \quad (4.3)$$

where

$$\mathbf{v}_{sr} = \begin{bmatrix} \mathbf{v}_s \\ \mathbf{v}_r \end{bmatrix}, \mathbf{f}_{sr} = \begin{bmatrix} \mathbf{f}_s \\ \mathbf{f}_r \end{bmatrix}, \mathbf{q}_{pf} = \begin{bmatrix} \mathbf{q}_p \\ \mathbf{q}_f \end{bmatrix} \quad (4.4,5,6)$$

and

$$\mathbf{M}_{sr} = \begin{bmatrix} \mathbf{M}_{s1} & \mathbf{M}_{s2} \\ \mathbf{M}_{r1} & \mathbf{M}_{r2} \end{bmatrix} \quad (4.7,8)$$

The dynamic response of the mounting system can be represented by its impedance matrix \mathbf{Z}_m and the internal secondary forces, so that

$$\mathbf{f}_m = \mathbf{Z}_m \mathbf{v}_m + \mathbf{q}_s \quad (4.9)$$

where \mathbf{f}_m is the vector of all 6 linear forces and moments at both ends of each mount \mathbf{v}_m is the corresponding vector of velocities at the ends of the mounts and \mathbf{q}_s is the vector of secondary forces acting within the mounts.

Referring to Fig. 4 we can see that when the source, mounts and receiving structure are connected, then

$$\mathbf{f}_m = -\mathbf{f}_{sr} \quad \text{and} \quad \mathbf{v}_m = \mathbf{v}_{sr}. \quad (4.10,11)$$

So the vectors of net forces and velocities acting at the junctions can be written in terms of the primary flanking and secondary forces as

$$\mathbf{f}_{sr} = \mathbf{Q}_{pf} \mathbf{q}_{pf} + \mathbf{Q}_{sf} \mathbf{q}_s, \quad \mathbf{v}_{sr} = \mathbf{Q}_{pv} \mathbf{q}_{pf} + \mathbf{Q}_{sv} \mathbf{q}_s \quad (4.12,13)$$

where

$$\mathbf{Q}_{pf} = -\mathbf{Z}_{m1} [\mathbf{I} + \mathbf{M}_{sr1} \mathbf{Z}_m]^{-1} \mathbf{M}_{sr2}, \quad \mathbf{Q}_{sf} = \mathbf{Z}_m [\mathbf{I} + \mathbf{M}_{sr1} \mathbf{Z}_m]^{-1} \mathbf{M}_{sr1} - \mathbf{I} \quad (4.14,15)$$

$$\mathbf{Q}_{pv} = [\mathbf{I} + \mathbf{M}_{sr1} \mathbf{Z}_m]^{-1} \mathbf{M}_{sr2}, \quad \mathbf{Q}_{sv} = -[\mathbf{I} + \mathbf{M}_{sr1} \mathbf{Z}_m]^{-1} \mathbf{M}_{sr1}. \quad (4.16,17)$$

Gardonio *et al* [7] have derived expressions for the full 6 degree of freedom mobility matrices for finite and infinite plates, to represent the receiving structure, of a rigid body, to represent the source structure, and distributed rods in which both flexural and compressional waves can propagate, to represent the elastomeric mounts. All the transfer responses in equations 4.12 and 13 can thus be calculated analytically and the effect of various control strategies can be evaluated in terms of the total power transmitted to the receiving structure, which can be written as

$$P_r = \frac{1}{2} \text{Re} (\mathbf{f}_r^H \mathbf{v}_r). \quad (4.18)$$

The effect on the total power transmitted to the receiving structure has been calculated when the secondary source is adjusted to minimise a variety of cost functions, J . All of these cost functions can be written as Hermitian quadratic functions of the secondary source amplitudes \mathbf{q}_s , so that in all cases

$$J = \mathbf{q}_s^H \mathbf{A} \mathbf{q}_s + \mathbf{q}_s^H \mathbf{b} + \mathbf{b}^H \mathbf{q}_s + c \quad (4.19)$$

which is minimised by the optimal vector of secondary source amplitudes given by

$$\mathbf{q}_s(\text{opt}) = -\mathbf{A}^{-1} \mathbf{b} \quad (4.20)$$

where \mathbf{A} and \mathbf{b} will depend on the form of the cost function being considered [7].

The results of such a calculation for the arrangement described in [7] are shown in Fig. 5. In Fig. 5(a) the transmitted power with no control is shown as the dark solid line, which has resonances associated with the mass spring resonances of the mounts, receiver and source system and those of the finite receiving structure and those of the mounts. The fainter solid line in Fig. 5(a) is the transmitted power if the secondary forces, which only act axially along the mounts, are optimally adjusted to minimise the total power supplied to the receiving structure (P_r). Good attenuation can thus be potentially achieved with these actuators at frequencies from about 10 Hz, which is the natural frequency of the main rigid body mode after control, to about 200 Hz, which is the frequency of a flexural resonance in the mount.

Fig. 5(b) shows the effect of canceling either the axial forces or axial velocities at the bottom of the mounts. The reduction in total transmitted power achieved by these strategies is surprisingly good, except at resonant frequencies of the controlled system. These frequencies are different for the cancellation of force or velocity, because of the different boundary conditions imposed by these two control strategies.

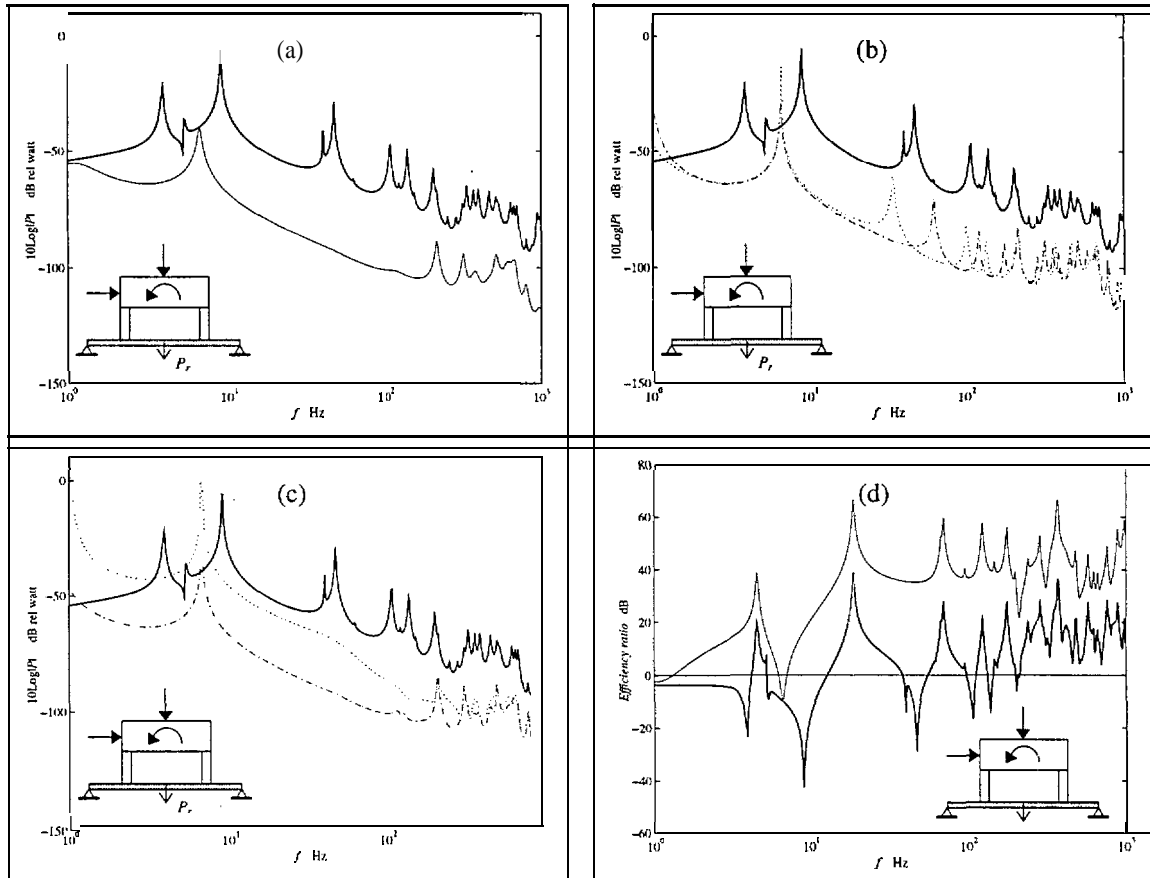


Fig. 5: Results of a computer simulation of the active isolation of a rigid body from a finite plate with two flexible active mounts which include axial force actuators. The total transmitted power with no active control (solid line), and with the actuators adjusted to minimise transmitted power (faint line) is shown in Fig. 5(a). The total transmitted power when the actuators are adjusted to minimise either the axial force (dotted line) or velocity (dot-dashed line) under the mounts is shown in Fig 5(b). The total transmitted power when the actuators are adjusted to minimise force \times velocity (J_1 , dotted line) or velocity²+force² (J_2 , dot-dashed line) are shown in figure 5(c). Fig. 5(d) shows the efficiency ratio (eqn 4.22) for the system with only passive isolation (solid line) and when the control actuators are adjusted to J_2 (faint line).

The dotted line in Fig. 5(c) shows the result of using the product of the axial force and velocity (J_1) as an estimate of the total transmitted power which is minimised by adjusting the secondary actuators. The reduction in total power is far less than when the system is optimally controlled, and at some frequencies is even significantly increased. This is due to the phenomena of *power circulation* in which the control system can minimise the power transmitted in the axial direction by increasing the transmission of power due to rotation, for example. This effect becomes even worse if an external flanking path is present and, together with the extreme sensitivity of this control strategies to phase errors in the transducers, this suggests that it would be very difficult to use such a cost function in practice. The result of minimizing the cost function equal to the sum of squared velocities and sum of squared forces (J_2) on total transmitted power is also shown in Fig. 5(c), and it can be seen

that the two sets of resonances, where either velocity or force could not be easily controlled in Fig. 5(b), have been avoided and when minimizing this combined cost function, the reduction in total transmitted power is close to the optimal levels shown in Fig. 5(a). Finally, the “efficiency” ratio of the passive and active isolation system, as used in earlier studies by Jenkins *et al* [8] and Pan *et al* [9], is shown in Fig. 5(d), which is defined here to be

$$E = \frac{P_r \text{ (rigid links)}}{P_r \text{ (passive or active mounts)}} \quad (4.22)$$

where P_r (rigid mounts) is the power transmitted to the receiving structure if the mounts are replaced by rigid links and the results for the active system have been evaluated when the new cost function (J_r) has been minimised. Although the ‘efficiency’ of the passive isolation system is small on average below 100 Hz and can become negative, the average ‘efficiency’ of the active system above about 10 Hz is nearly 40 dB.

4. Experimental Study

The experiments were conducted using the active isolator arrangement shown in Fig. 6. The source structure consisted of a rigid 200 x 100 x 18 mm block of aluminium on which two electromagnetic shakers were mounted, which had a total mass of about 3 kg.

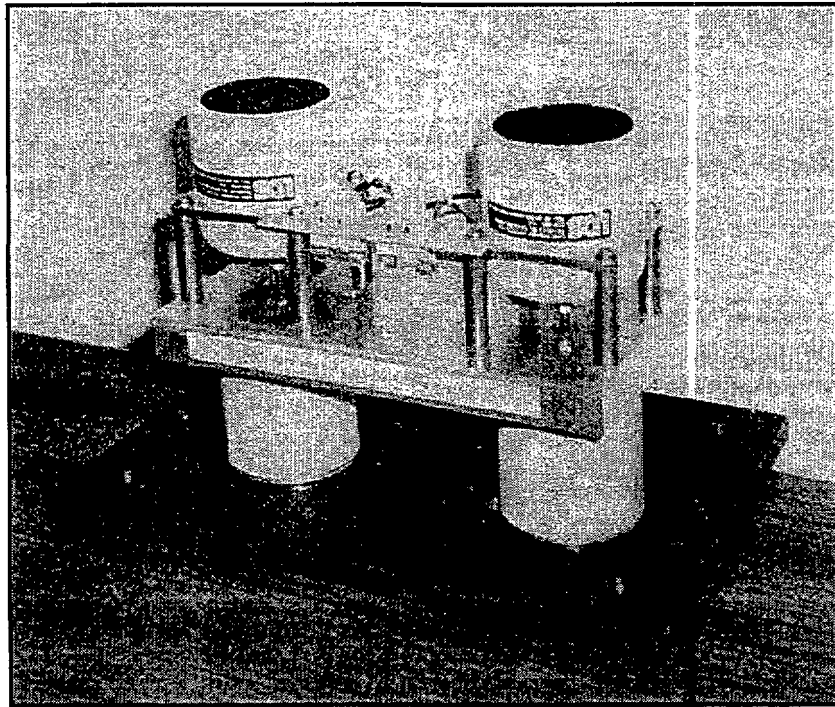


Fig. 6: The active isolator.

The isolators were soft rubber rings of height 60 mm, internal diameter 40 mm and external diameter 60 mm. The receiving structure is shown in Fig.7, and was a 15 mm thick Perspex plate, rigidly mounted in a wall between two reverberant rooms, which had grooves cut into it so that it behaved approximately like a simply supported plate of dimensions 890 x 790 mm.

20 miniature accelerometers were also mounted on the plate so that its total kinetic energy could be estimated from the sum of the squared outputs of these devices.

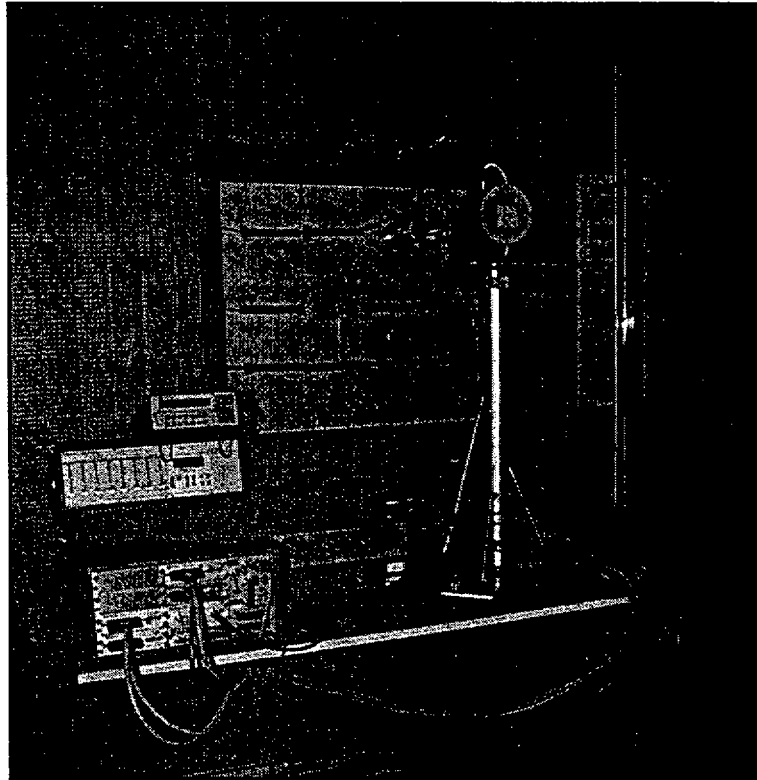


Fig 7: *Experimental set up.*

Three matched force sensors (B+K 8200) were placed under each mount to measure only the axial force, together with an accelerometer (B+K 4375) whose output was integrated to provide a measure of axial velocity.

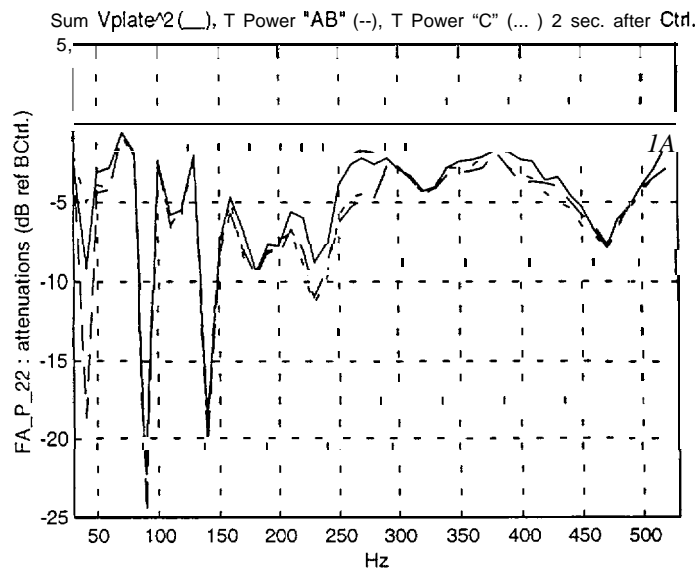


Fig 8: *Attenuation in the sum of squat-cd velocities measured at 20 positions on the receiving plate (solid line) and attenuations in the measured estimate of transmitted power (dashed line) when the measured transmitted power was minimised at a number of discrete frequencies using a real-time control system.*

Some of the results of these experiments are shown in Fig. 8 in which the attenuation in the transmitted power measured using the force gauges and accelerometers under the mount, are compared with the attenuations in the estimated kinetic energy of the receiving plate, for an experiment in which measured transmitted power was minimised. The similarity between these two graphs shows that minimizing the excitation of the receiving plate does lead to commensurate reductions in the response of this plate.

6. **Conclusions**

The main conclusions of this study are:

- i) That total power transmission is a powerful criterion for evaluating different active vibration control strategies, particularly in theoretical studies.
- ii) There are significant practical problems with minimizing a direct estimate of transmitted power, obtained by multiplying forces and velocities, because of “power circulation” and the extreme sensitivity to transducer phase errors.
- iii) That a new cost function which indirectly estimates the transmitted power by taking a weighted sum of squared velocities and forces does not suffer from these problems and appears to give near-optimal results.
- iv) That this new control strategy can be readily programmed into a feedforward control system and gave good results in an experimental investigation.

7. **Acknowledgements**

This work was supported under the EC Brite-Euram project Active Control of Structural vibration using Power Transmission Methods (ASPEN), Contract Number BRE2-CT93-0548. Project Number BE7228.

REFERENCES

1. G. Pavic (1995) *Comparison of different strategies for active vibration control*. Proc. Active 95, p. 197-208.
2. O, Bardou, P. Gardonio, S. J.Elliott and R. J. Pinnington (1997) *Active power minimisation and power absorption in a plate with force and moment excitation*. To be published in the Journal of Sound and Vibration.
3. P. A. Nelson, M.D. Jenkins and S. J.Elliott (1987) *Active isolation of periodic vibrations*. Proc Noise-con 87, Penn State University, p.425-430.
4. J. Garcia-Bonito et al (1997) *Design of actuators for active vibration control*. ISVR Contract Report 97/05.

5. A. David *et al* (1997) *Final report on the design and testing of an active vibration isolator*. ISVR Contract Report 97/
6. S.Laugesen (1994) *An example of power-based active control of vibration*. Proc. IUTAM Symposium. Active Vibration, Control of Vibration.
7. P. Gardonio *et al* *Journal of Sound and Vibration* (1) *Active isolation of structural vibration on multiple degree of freedom systems. Part I: Dynamics of the system* and (2) *Active isolation of structural vibration on multiple degree of freedom systems. Part II: Active control strategies effectiveness*. To be published.
8. M. Jenkins, P. A. Nelson, R. J. Pinnington and S. J.Elliott (1993) *Active isolation of periodic machinery vibrations*. *Journal of Sound and Vibration* 166, p. 117-140.
9. J.Pan, J Pan and C. H. Hansen (1992) *Total powerflow from a vibrating rigid body to a thin panel 27/04/97 19:12 through multiple elastic mounts*. *Journal of the Acoustical Society of America*, 92, p.895-907.